

Communication

Molecular-orientation analysis based on alignment-induced TROSY chemical shift changes

Shin-ichi Tate^{a,*}, Hideto Shimahara^b, Naoko Utsunomiya-Tate^c

^a Department of structural biology, Biomolecular Engineering Research Institute (BERI), 6-2-3 Furuedai, Suita, Osaka 565-0874, Japan

^b Center for New Materials, Japan Advanced Institute of Science and Technology (JAIST) 1-1 Asahidai, Tatsunokuchi, Ishikawa 923-1292, Japan

^c Department of Veterinary Science, Nippon Veterinary and Animal Science University, 1-7-1 Kyouunan-cho, Musashino-shi Tokyo 180-8602, Japan

Received 17 May 2004; revised 3 September 2004

Available online 2 October 2004

Abstract

We present a new NMR technique for determining the alignment tensor of a weakly aligned protein using only alignment-induced ¹⁵N transverse relaxation optimized spectroscopy (TROSY) chemical shift changes. Alignment-induced TROSY chemical shift changes reflect the combined contributions from two different anisotropic spin interactions including the residual dipolar couplings (RDCs) and the residual chemical shift anisotropy effects (RCSAs). We show here that these two residual anisotropic spin interactions' values, encoded in the TROSY chemical shift changes, can be used to determine a weakly aligned protein's alignment tensor. To prove the significance of this method, we show that our TROSY-based analysis gives the consistent alignment angles with those determined using RDCs for ¹⁵N-labeled ubiquitin (8.6 kDa) in an aligned medium, within an uncertainty range estimated by considering experimental and structural noises, being 5° at most. Because our approach requires a pre-determined ¹⁵N CSA tensor value, we also estimated the uncertainties associated with the resultant alignment tensor values caused by variation in ¹⁵N CSA tensors. In spite of the significant variations in literature-reported ¹⁵N CSA tensors, they gave consistent orientation angles within an uncertainty range. These results ensure that our TROSY-based approach is a useful alternative to the RDC-based method to determine the alignment angles especially for large proteins in a weakly aligned state.

© 2004 Elsevier Inc. All rights reserved.

Keywords: Residual dipolar coupling; TROSY; Weak alignment of a protein; Chemical shift anisotropy; Magic angle sample spinning

1. Introduction

The inclusion of anisotropic spin interactions in macromolecular solution NMR experiments provides useful techniques for protein structure analysis [1–5]. The residual dipolar coupling (RDC), associated with a spin pair of a weakly aligned protein, contains information about the relative orientation of the pair's internuclear vector relative to the molecule's alignment frame. Use of the RDCs in structure calculations improves the local geometry [6] and also provides a unique opportunity for structure validation [7]. A notable RDC application,

which gives global structural information by incorporating all bond vectors into a single alignment axis system, is the determination of the relative orientation of domains or subunits in a protein [8,9]. For this application, starting with the X-ray coordinates of a protein, the RDCs are then used to reorient domains or subunits and, by doing so, the technique provides a rapid means of establishing an average solution structure of a multi-domain or multi-subunit protein. This RDC-based approach is useful when determining the solution structures of large proteins composed of domains or subunits, and especially when the quantitative elucidation of a structural change caused by, for example, ligand binding is sought. However, the presently available experiments to measure the RDC [10–12], which are

* Corresponding author. Fax: +81 6 6872 8210.

E-mail address: tate@beri.or.jp (S.-i. Tate).

all basically F_1 -coupled HSQC spectroscopy, should not be applied to multiple-domain proteins or proteins composed of subunits that have a molecular weight of typically more than 40 kDa. This molecular weight limitation is the practical drawback for RDC experiments when attempting to assess the relative orientations of a protein's domains or subunits.

For large proteins, the upfield $^{15}\text{N}\{-^1\text{H}\}$ doublet component in an F_1 -coupled HSQC spectrum is broadened to reduce spectral resolution and its intensity is concomitantly weakened as a result of interference between $^1\text{H}\text{-}^{15}\text{N}$ dipolar coupling and ^{15}N chemical shift anisotropy relaxation mechanism [13]. On the other hand, the downfield $^{15}\text{N}\{-^1\text{H}\}$ doublet component remains sharp and intense even in the spectra of large proteins. This downfield component is the ^1H -coupled analogue, along ^1H dimension, to that which is observed in TROSY experiments, where the narrowest of the four possible heteronuclear-multiplet components is selected [14]. Because the RDC is measured by the alignment-induced modulation to $^1J_{\text{NH}}$ appearing as difference in frequency between the doublet components in a F_1 -coupled HSQC spectrum, the rapid transverse relaxation of the upfield doublet component severely limits the accuracy of the RDCs for large proteins.

To remedy this problem, Kontaxis et al. [15] measured the RDCs using the difference in the ^{15}N frequency of each correlation signal found for TROSY and F_1 -decoupled HSQC spectra. For an F_1 -decoupled HSQC spectrum, the ^{15}N transverse relaxation rate of each correlation signal is roughly an average of the corresponding doublet's rates in the F_1 -coupled $^1\text{H}\text{-}^{15}\text{N}$ HSQC spectrum; thus the upfield component's adverse effect is alleviated for the F_1 -decoupled HSQC spectrum. The combined use of the TROSY and F_1 -decoupled $^1\text{H}\text{-}^{15}\text{N}$ HSQC spectra was successfully applied to the measurement of the RDCs for proteins over 40 kDa when determining the relative orientation of protein domains and subunits [8,9]. However, the more rapid ^{15}N relaxation of the F_1 -decoupled HSQC signals, compared with those of the TROSY signals, will limit the accuracy of the RDCs for proteins of molecular weight greater than 100 kDa; for such proteins, only the TROSY experiment provides a spectrum with the necessary resolution and sensitivity.

Two relating 3D TROSY-HNCO-based methods that scale the position of the upfield $^{15}\text{N}\{-^1\text{H}\}$ double component, with simultaneously alleviating the rapid transverse relaxation of the component, (J -scaling) are used to accurately measure the various types of RDCs for proteins ranging 30–40 kDa [15,16]. These methods are also basically the ^1H -coupled HSQC in respect to measuring the RDC for $^1\text{H}\text{-}^{15}\text{N}$ spin pair. Therefore, their application to much higher molecular weight proteins will be limited.

Here, we present a new approach for determining a protein's alignment angles, which uses only the align-

ment-induced changes of ^{15}N TROSY signals. We show that changes in the alignment-induced TROSY chemical shifts give consistent alignment angles compared with those determined by the RDCs within an uncertainty range that accounts for experimental uncertainties and structural noises. This comparison ensures that our TROSY-based approach is valid when determining the molecular alignment angles for much larger proteins; for those cases, only TROSY spectroscopy will be applicable.

2. Method

The alignment-induced TROSY ^{15}N chemical shift changes are influenced by two anisotropic interactions—the RDC and the residual ^{15}N chemical shift anisotropy (RCSA). ^{15}N chemical shift anisotropy (CSA) is the result of anisotropic magnetic shielding around the backbone amide ^{15}N nucleus; thus, the RCSA appears as a peptide plane orientation-dependent change to the ^{15}N chemical shift. Fig. 1 schematically depicts the apparent alignment-induced $^1J_{\text{NH}}$ modulation, which is used to measure the RDC. When compared with the downfield component, the upfield $^{15}\text{N}\{-^1\text{H}\}$ doublet component (the anti-TROSY component) has a shorter transverse relaxation time due to interference between the ^{15}N CSA and the one-bond $^1\text{H}\text{-}^{15}\text{N}$ dipolar interaction [13]. This upfield doublet

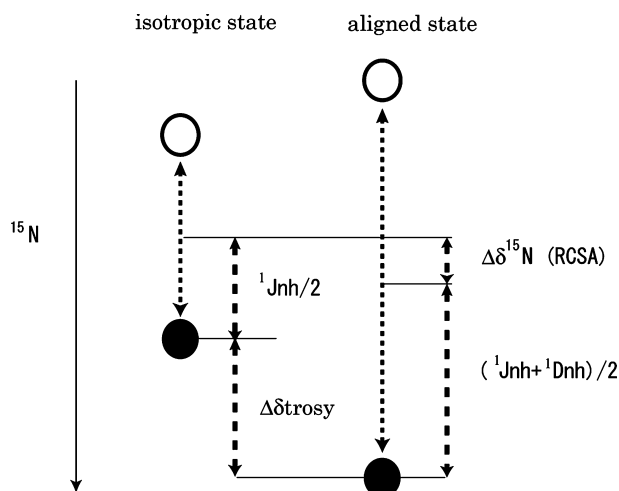


Fig. 1. A schematic of the relationship among the observables for the $^{15}\text{N}\{-^1\text{H}\}$ doublet in a F_1 -coupled HSQC spectra, observed in the isotropic and the aligned states. The open and closed circles represent the anti-TROSY and the TROSY doublet component, respectively. $^1J_{\text{NH}}$ is the one-bond scalar coupling between ^1H and ^{15}N . $\Delta\delta^{15}\text{N}$ is the chemical shift change in a F_1 -decoupled HSQC spectrum induced by the orientation of the peptide plane against the magnetic field. $\Delta\delta_{\text{TROSY}}$ is the orientation-dependent chemical shift change to the TROSY doublet component. As diagramed, $\Delta\delta_{\text{TROSY}}$ involves incomplete cancellation of ^{15}N chemical shift anisotropy and residual dipolar coupling, $^1D_{\text{NH}}$, one-half of which contributes to the $\Delta\delta_{\text{TROSY}}$.

component, shown by an open circle, is difficult to measure for spectra of large proteins. As shown on the right-hand side of Fig. 1, the alignment-induced chemical shift change for the downfield TROSY component, $\Delta\delta_{\text{TROSY}}$, involves both the RDC and the RCSA, according to the following relationship:

$$\Delta\delta_{\text{TROSY}} = \text{RDC}/2 + \text{RCSA} \quad (1)$$

When determining the alignment tensor of a protein using its known structure, the RDC and the RCSA for each ^1H – ^{15}N spin pair are readily calculated from the structure's coordinates. For each ^1H – ^{15}N nuclear spin pair, k , Eq. (1) can be rewritten with Saupe order matrix elements [17] as

$$\Delta\delta_{\text{TROSY}}(k) = \sum_{i,j=x,y,z} S_{ij} \{0.5D_{\text{NH}}^0 \cos \phi_i^k \cos \phi_j^k + (2/3)\delta_{ij}^k\}, \quad (2)$$

where ϕ_i^k is the angle of the NH bond vector for the k th spin pair relative to the i th molecular axis and δ_{ij}^k is the element of the chemical shift tensor for the k th ^{15}N nucleus expressed in an arbitrary molecular frame [17,18]. S_{ij} is the Saupe order matrix element that defines the molecular alignment relative to the magnetic field [17]. D_{NH}^0 is the static dipolar coupling, which equals 23.0 or 21.7 kHz for assumed NH bond lengths of 1.02 or 1.04 Å, respectively. The latter is the vibronically corrected bond length, and is proposed to be an appropriate estimate of the NH bond length for proteins in solution [19]. When the ^{15}N CSA tensors, each of which is associated with a δ_{ij}^k element in Eq. (2), are known for all of the ^{15}N nuclei, the Saupe order matrix can be obtained by singular value decomposition (SVD) calculations [18].

The ^{15}N CSA tensor is sensitive to local spin interactions arising from, for example, conformation, solvation, and/or hydrogen bonding states [20]. Thus, the value for each residue's ^{15}N CSA tensor is hard to know a priori. Therefore, in the present analysis, for a given calculation of the alignment tensor, we used single ^{15}N CSA tensor with assuming that the values for all residues' ^{15}N CSA tensors were the same.

3. Results

We used the spectra of ^{15}N -labeled human ubiquitin, dissolved in a 7.5% (w/v) DMPC/DHPC/CTAB bicelle-containing medium with 0.5 mM protein concentration, to measure RDC and alignment-induced TROSY chemical shift changes.

In previous work, we determined the ^{15}N CSA tensor value for ^{15}N ubiquitin in solution using the high-resolution magic angle sample spinning (HR-MAS) [21]. At first in the present analysis, we used this tensor value determined for the same sample. Our previously re-

ported ^{15}N CSA tensor values were determined using the 1.8 Å X-ray structure of ubiquitin [22]. For the present analysis, we re-determined the values with the NMR structure refined by using dipolar couplings [23]. The updated ^{15}N CSA tensor values are listed in Table 1, results a and b. The uncertainties for the CSA values were estimated in the Monte-Carlo manner with considering imprecision in measuring peak position and structural noise coming from local NH bond vibration [21,24]. Two NH bond lengths of 1.02 Å (result a) and 1.04 Å (result b), respectively, were used to determine the CSA values [21] to consider any effects caused by different NH bond lengths in the subsequent analyses.

To obtain the accurate orientation-dependent ^{15}N TROSY shifts, $\Delta\delta_{\text{TROSY}}$, we recorded a set of ^1H – ^{15}N TROSY spectra measured with and without magic angle sample spinning (MAS) on a 500 MHz NMR spectrometer equipped with a NanoProbe (Varian) [21,25,26]. The application of the MAS to an ordered bicelle medium eliminates the torque that aligns the bicelles against the magnetic field [26]. Thus, the anisotropic spin interactions, which include the RDC and the RCSA, are eliminated while all other experimental conditions are kept the same [21]. As chemical shift is very sensitive parameter to sample conditions, the application of the MAS substantially improved the accuracy of the $\Delta\delta_{\text{TROSY}}$.

The calculated principal components and the Euler angles for the alignment tensor and their associating uncertainties are listed in Table 1 (results a and b); the uncertainties were also estimated by the Monte-Carlo method with both measuring imprecision and structural noises considered [24]. In the alignment tensor calculation, the ^{15}N CSA values and their associated uncertainties, estimated in the Monte-Carlo manner, were considered. The difference in the anisotropy parameter, $\Delta\sigma$, caused by different NH bond lengths mainly affected the alignment tensor magnitudes, but had little effect on the orientation angles' values (Table 1, results a and b). In both cases, the orientation angles are consistent with those determined by the RDCs from the IPAP-HSQC experiments within an estimated uncertainty range (Table 1, result i). The results show that our TROSY-based approach, with assuming the unique ^{15}N CSA tensor value for all backbone ^{15}N nuclei in a protein, yields the consistent orientation angles for an aligned protein with those calculated from the RDCs independent of the assumed NH bond length.

The quality factors (Q -factors in Table 1) for the determined alignment tensors were 0.43 ± 0.04 in both cases using different NH bond lengths (Table 1, results a and b). These less excellent values come from the consideration of noises, particularly structural noises that were involved in both the ^{15}N CSA tensor determination and the subsequent alignment tensor calculation from the $\Delta\delta_{\text{TROSY}}$. Without considering the noises in the

Table 1

Alignment tensor magnitudes and orientations in ^{15}N labeled ubiquitin determined from $\Delta\delta_{\text{TROSY}}$ values with various ^{15}N CSA tensors

Results [ref.]	$\Delta\sigma$ (ppm) ^A	η ^B	β (°) ^C	A_{zz} (10^{-4}) ^D	A_{yy} (10^{-4})	A_{xx} (10^{-4})	Euler angles (°) ^E			Q-factor ^F
							α	β	γ	
a [21]	-168.1 ± 4.3	0.19 ± 0.02	17.7 ± 0.5	-9.48 ± 1.89	7.79 ± 1.56	1.69 ± 0.40	82.1 ± 4.9	74.0 ± 2.4	72.9 ± 2.9	0.43 ± 0.04
b [21]	-158.5 ± 4.1	0.19 ± 0.02	17.7 ± 0.5	-10.10 ± 1.90	8.30 ± 1.57	1.80 ± 0.41	82.0 ± 4.5	73.9 ± 2.3	72.8 ± 2.8	0.43 ± 0.04
a' [21]	-166.9	0.19	17.7	-10.66	8.82	1.85	80.9	73.2	73.0	0.29
b' [21]	-157.5	0.19	17.7	-11.30	9.35	1.96	80.9	73.2	73.0	0.29
a'' [21]	-166.9	0.19	17.7	-10.77	8.67	2.10	79.0	75.7	71.3	0.38
b'' [21]	-157.5	0.19	17.7	-11.42	9.19	2.23	79.0	75.7	71.3	0.38
c [30]	-162.5	0.19	20.0	-10.98	9.03	1.95	81.4	73.3	72.8	0.27
d [29]	-174.4	0.15	18.7	-11.70	9.56	2.14	82.2	73.3	72.7	0.27
e [32]	-168.8	0.22	24.5	-10.07	8.22	1.84	82.0	73.4	72.5	0.27
f [33]	-151.5	0.02	18.6	-10.83	9.03	1.80	80.8	73.6	73.8	0.31
g [31]	-164.4	0.06	22.0	-10.53	8.68	1.85	81.8	73.6	73.3	0.29
h	-164.3 ± 8.5	0.13 ± 0.09	20.8 ± 2.5	-10.82 ± 0.60	8.90 ± 0.50	1.92 ± 0.14	81.6 ± 0.6	73.4 ± 0.1	73.0 ± 0.5	0.28 ± 0.02
i				-13.28 ± 0.27	10.98 ± 0.27	2.29 ± 0.15	82.5 ± 1.3	74.9 ± 1.0	74.9 ± 1.0	0.14 ± 0.01
j				-5.98 ± 0.15	5.20 ± 0.14	0.78 ± 0.08	75.8 ± 1.5	74.8 ± 1.2	73.3 ± 1.3	0.55 ± 0.02

The rmsd values for results a, b, and i were evaluated from a 500 step Monte-Carlo simulation, with a rms noise level of 0.34 Hz, which corresponds to the uncertainty for measuring peak positions in a TROSY spectrum, which uncertainty was estimated from the pairwise rms deviation of the observed shifts in the two TROSY spectra collected sequentially. The structural noise that assumes a random distribution of each NH bond vector within a cone with 5° tilt angle [24].

For results a and b, the alignment tensors were calculated using ^{15}N CSA values determined under the same conditions used in the present work [21]. Results for a' and b' were estimated from the optimal ^{15}N CSA tensor values without considering the measuring error and structural noise. NH bond lengths of 1.02 and 1.04 Å were used in results a (a') and b (b'), respectively. Results c–g were obtained using various ^{15}N CSA values reported in literatures [29–33]. Result h reports the average and the deviation for the input ^{15}N CSA values and the resultant alignment tensors listed in results c–g. Result i shows the alignment tensor determined from the IPAP-HSQC experiments assuming NH bond length of 1.04 Å.

Results a'' and b'' show the alignment tensor parameters determined using the X-ray structure of ubiquitin [22]. Proton positions were added to the crystal structure using the program MOLMOL [40]. To compare the alignment angles, α , β , and γ , with those determined by using the NMR structure, the X-ray coordinate was rotated to gain the maximal overlay to the NMR structure at the backbone atoms of residues 3–72 with omitting the flexible terminal residues [27], which residues were used in the alignment tensor analysis.

Result j shows the alignment tensor parameters determined from the values of $\Delta\delta_{\text{TROSY}}$ multiplied by 2, which values are assumed to be approximate RDCs in this calculation to assess the significance of the RCSA contribution to the $\Delta\delta_{\text{TROSY}}$.

^A $\Delta\sigma = \sigma_{11} - (\sigma_{22} + \sigma_{33})/2$. σ_{11} , σ_{22} , σ_{33} values are the ^{15}N CSA tensor components.

^B $\eta = [(\sigma_{\text{int}} - \sigma_{\text{min}})/\sigma_{\text{max}}]$, where the subscripts maximum (max), minimum (min), and intermediate (int) refer to the absolute magnitudes of σ_{11} , σ_{22} , σ_{33} .

^C The angle β is defined as the angle between the σ_{11} axis and the NH bond in a peptide plane.

^D A_{xx} , A_{yy} , and A_{zz} are the principal components of the alignment tensor. In the diagonalized traceless molecular alignment tensor frame, Eq. (2) is expressed as $\sum_{i,j=x,y,z} A_{ii}(0.5D_{\text{NH}}^0 \cos^2\phi_i + \cos^2\theta_{ij}\delta_{jj})$ where ϕ_i is the angle between the NH bond vector and the A_{ii} principal axis of the alignment tensor, θ_{ij} is the angle between the δ_{jj} principal axis of the traceless CSA tensor and the A_{ii} principal axis of the molecular alignment tensor.

^E The Euler angles α , β , and γ define the alignment tensor orientation relative to the coordinate frame of the NMR structure of ubiquitin refined with dipolar couplings [23].

^F Quality factors are defined separately for the $\Delta\delta_{\text{TROSY}}$ and RDC-based analyses. For the $\Delta\delta_{\text{TROSY}}$ -based alignment tensor determination, the quality factor was defined in analogy with that proposed by Cornilescu et al. $Q = \{[\sum(\Delta\delta_{\text{TROSY}}(\text{obs.}) - \Delta\delta_{\text{TROSY}}(\text{calc.}))^2]^{1/2} / \{[\sum(\Delta\delta_{\text{TROSY}}(\text{obs.})^2)]^{1/2}\}$ [23]. The quality factor for the RDC-based analysis is defined in the same manner as $\{[\sum(^1D_{\text{NH}}(\text{obs.}) - ^1D_{\text{NH}}(\text{calc.}))^2/N]^{1/2} / \{[\sum(^1D_{\text{NH}}(\text{obs.})^2/N)]^{1/2}\}$, where $^1D_{\text{NH}}$ denotes the RDC and N is the number of data used. In the present evaluation, due to the non-uniform distribution of the NH bond vector orientation in ubiquitin [41], we used $\{D_a^2[4 + 3(D_r/D_a)^2]/5\}^{1/2}$ as denominator of the formula with the axial and rhombic components of the alignment tensor, D_a and D_r [42].

TROSY-based alignment tensor determination, the quality factors were 0.29 for both NH bond lengths (Table 1, results a' and b'). It should be noted, the same TROSY-based analyses using the X-ray structure [22] gave worse quality factors, 0.38, for both bond lengths without considering noises (Table 1, results a'' and b''). This shows that the quality factor is very sensitive to the subtle difference in the structure used for the tensor determination; the room mean square deviation of backbone N, C α , C', HN atoms between the X-ray and the dipolar refined NMR structures is 0.35 Å for residues 13–72, which residues were used in the present analyses with omitting flexible terminal residues [27]. Although

the quality factor became worse, the alignment angles determined with the X-ray structure were still consistent with those by the NMR structure within an error range (Table 1, results a, b, a'', and b''). This shows that the TROSY-based alignment analysis does not necessary require the RDC refined structure to obtain the alignment angles within an intrinsic uncertainty given by the method, which determines the angles within 5° at most in considering possible experimental and structure noises.

The quality factors for the tensors from $\Delta\delta_{\text{TROSY}}$ (Table 1, results a' and b') are worse than that from the RDCs (Table 1, result i). This discrepancy may partly occur from the assumption of the unique ^{15}N

CSA tensor value to all residues. To access the bias caused by neglecting local variation in ^{15}N CSA tensor, we tried the TROSY-based analysis with incorporating the residue specific ^{15}N CSA tensor values determined for ubiquitin by ^{15}N spin relaxation analysis [28]. The relaxation analysis does not give a complete set of ^{15}N CSA tensor parameters for each residue, but it gives only anisotropy ($\Delta\sigma$) and the angle (β) between the unique principal axis, σ_{11} , and the NH bond; the asymmetry parameter, η , is not available [28]. In the present assessment, we assumed the unique η for all residues with using the residue specific $\Delta\sigma$ and β values from the ^{15}N relaxation analysis. We systematically varied η from 0.04 to 0.22 by the step of 0.03 to seek the optimal η value, but the resultant quality factors were all 0.33 in this range of the η variation. Without associating knowledge of η , no significant improvement in the quality factor was obtained by incorporating the residue specific ^{15}N CSA tensor values.

Major reason to the worse quality factors for the TROSY-based alignment tensors should come from the smaller absolute value of $\Delta\delta_{\text{TROSY}}$ than the corresponding RDC. In the TROSY-based alignment, only a half of the RDC is considered, Eq. (1). The RCSA shows mostly opposite sign to the RDC, Fig. 2A. Therefore, the $\Delta\delta_{\text{TROSY}}$ value is overall less than a half of the RDC. Formulae to define the quality factors are described at the bottom of Table 1 for the alignment tensors determined by the RDC- and the TROSY-based analyses, respectively. According to the formulae, the reduction by half of the absolute observed values doubles the value of the quality factors, even in the same extent of the discrepancies between the observed and the back-calculated values. Therefore, the difference in the quality factors for the RDC and the $\Delta\delta_{\text{TROSY}}$ derived alignment tensors is mainly ascribed to the different absolute magnitudes of the alignment-induced modulation to these two experimental values. In spite of the worse quality factor for the $\Delta\delta_{\text{TROSY}}$ derived alignment tensor than that for one from the RDCs, it is worthy of note that the orientation angles are close to those obtained from the RDC experiments; i.e., the results are consistent within an uncertainty (Table 1, results a', b', and i).

The RDC contribution to the $\Delta\delta_{\text{TROSY}}$ is indeed greater than that of the RCSA overall, even a half of the RDC is considered. But this is not always the case. The unique principal axis of the ^{15}N CSA, σ_{11} , is apart from the NH bond vector by 17.7° (Table 1, results a and b). Because of their different orientations in peptide plane, while a NH bond directs in the magic angle against the magnetic field, resulting in no apparent RDC observed, the corresponding RCSA shows significant values. Therefore, although the overall profiles of the RDC and the RCSA along the residue look similar, Fig. 2A, the ratios of their contribution to the $\Delta\delta_{\text{TROSY}}$

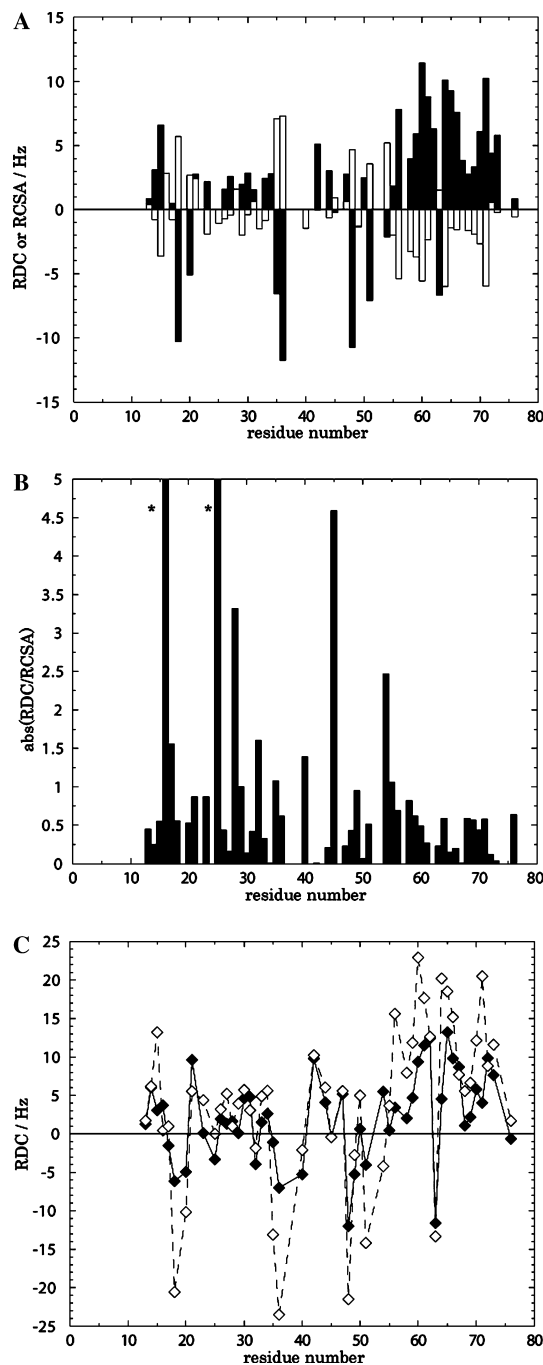


Fig. 2. (A) Plot of the RDC/2 (black bar) and the RCSA (open bar) values contributing to each $\Delta\delta_{\text{TROSY}}$ along the residue number. (B) Absolute ratios of the magnitude of the RCSA to that of the RDC/2 for each residue are plotted along the residue number. The ratios for the residues 16 and 25 were out of the vertical range, shown with asterisks; they were 12.8 and 107.0 for the residues 16 and 25, respectively. (C) The RDC values observed in the IPAP experiment (open diamond) and the values of the alignment-induced TROSY shifts multiplied by 2, $2\Delta\delta_{\text{TROSY}}$, (black diamond) are plotted along the residue number.

are not constant for the residues. Fig. 2B plots the ratio of the absolute magnitude of the RCSA to the RDC/2 for each residue. Residues 16 and 25 show extremely

large values due to the small RDCs; for these residues, the NH bonds are directing to near the magic angle. The average ratio for the residues except these two, residues 16 and 25, was 0.70 ± 0.42 . As seen in Fig. 2B, although the RCSA contribution to the $\Delta\delta_{\text{TROSY}}$ is less than that of the RDC on average, it is not ignored to obtain the accurate molecular alignment angles. To access the significance of the RCSA contribution to the $\Delta\delta_{\text{TROSY}}$, we calculated the alignment tensors with neglecting the RCSA term in the $\Delta\delta_{\text{TROSY}}$, Eq. (1); where the RDC is simply estimated as the value of the $\Delta\delta_{\text{TROSY}}$ multiplied by 2. The RDC values obtained from the IPAP experiment and the $2\Delta\delta_{\text{TROSY}}$ values, which are the assumed RDCs in neglecting the RCSA contribution, are plotted along the residues, Fig. 2C. Overall, the $2\Delta\delta_{\text{TROSY}}$ values are underestimated in magnitudes than the real RDC values. The determined alignment tensor values based on the $2\Delta\delta_{\text{TROSY}}$ are listed in Table 1, result j. The obtained alignment angles were not consistent with those derived from the RDCs (Table 1, results i and j). The quality factor for the determined tensor became severely worse than that for the RDC derived tensor (Table 1, results i and j). From this assessment, the contribution of the RCSA is significant to obtain the accurate alignment tensor values. Thus, the simultaneous incorporation of the RDC and the RCSA in the alignment tensor determination from the $\Delta\delta_{\text{TROSY}}$, Eq. (2), is essential.

To further validate the TROSY-based alignment tensor determination, we explored the effect of varying the ^{15}N CSA tensor values on the resultant alignment tensors. A variety of NMR experiments have reported rather different ^{15}N CSA values [21,29–33]. The variations in the reported ^{15}N CSA values may represent its changes caused by through-bond substituent effects, conformational effects, and/or effects arising from interaction with the surroundings, as suggested by quantum-chemical calculations [20]. Unless the ^{15}N CSA values are determined with the same sample used for the TROSY experiments, the ^{15}N CSA values must be obtained from literatures. Considering that this is often the case, it is practically important to assess how different ^{15}N CSA values affect the resulting alignment tensors in our TROSY-based approach. The values for ^{15}N CSA tensors in literature and the corresponding calculated alignment tensors with using 1.04 Å NH bond length are listed in Table 1, results c–g. Comparing these results shows that the resultant alignment tensor angles are rather insensitive to the variations in the values of the ^{15}N CSA tensors. The average tensor values for the results c–g are listed in Table 1, result h. In particular, the alignment angles are within an estimated uncertainty of the result b in Table 1. This comparison demonstrates that the variation in the literature reported ^{15}N CSA tensor has limited effect on the orientation angles determined by the $\Delta\delta_{\text{TROSY}}$; although, a somewhat

larger variation in the alignment tensors' magnitudes is noted. Therefore, in the TROSY-based analysis, any reported ^{15}N CSA value will yield the consistent alignment angles with those derived from the RDCs.

In comparing the quality factors for results a' and b' in Table 1 with those listed in the results c–g, it is noted that our reported ^{15}N CSA values derived from the HR-MAS experiments [21] did not show the best fitting quality. This does not mean that the HR-MAS derived ^{15}N CSA values are less accurately determined. Because the $\Delta\delta_{\text{TROSY}}$ -based alignment tensor analysis uses unique ^{15}N CSA values for all residues neglecting their intrinsic local variations, it is reasonable that the best determined average ^{15}N CSA values over the sampled residues do not always provide the best fit in the TROSY-based alignment analysis. As shown in the results a and b in Table 1, the experimental and structural noises cause more reduction in the fitting quality but the alignment angles coincide with those from the RDCs within an error range (Table 1, result i). The quality of the determined alignment tensors is much more influenced by the structure noises representing local NH-bond vibration and the experimental imprecision in recoding the peak positions than the variation in the input ^{15}N CSA tensor values. It is the point that the range of the quality factors exemplified in the Table 1, results a', b', and c–g, are all acceptable within an uncertainty intrinsically imposed by the TROSY-based analysis.

4. Conclusions

In this communication, we provide an alternative approach to calculate the alignment tensor for a weakly aligned protein, which approach uses the orientation-dependent ^{15}N TROSY chemical shift changes, $\Delta\delta_{\text{TROSY}}$. We show that the orientation angles obtained from this TROSY-based analysis are consistent with those determined using the RDCs within an error range estimated by considering the experimental and the structure noises (Table 1, results a, b, and i). Although our approach requires a pre-determined ^{15}N CSA tensor value, which are intrinsically sensitive to both the local structure and the local environment of a protein, we found that any of the ^{15}N CSA tensor values in literature gave the consistent orientation angles with those determined by using the experimentally determined ^{15}N CSA tensor for the same sample (Table 1, results a, b, and c–g). In our TROSY-based approach, the ^{15}N CSA values are assumed to be unique for all residues in protein, but this assumption does not limit the accuracy of the resultant alignment tensor values. In comparing the results obtained by using the X-ray structure and the dipolar refined NMR structure, both gave also the consistent alignment angles, although the significant reduction in the fitting quality was found in using the X-ray

structure. Therefore, this TROSY-based alignment tensor analysis is widely applied to the orientation analysis of structure known proteins without any further structure refinement and any specific knowledge of the ^{15}N CSA tensor values to each protein; this approach ensures the uncertainties for the alignment angles 5° at most.

This method overcomes the difficulty in measuring RDCs from F_1 -coupled HSQC spectra of large proteins where the upfield ^{15}N - $\{^1\text{H}\}$ doublet component is weak or absent. A TROSY spectrum has higher resolution and sensitivity relative to the corresponding HSQC spectrum, especially for proteins greater than 100 kDa [34,35]. The TROSY-based orientation analysis presented here takes full advantage of the TROSY spectroscopy's spectral resolution and sensitivity for extremely large proteins. Our approach may provide a useful NMR tool for quantitative analyses of domain or quaternary structure rearrangements for pharmaceutically interesting proteins that have a molecular weight that precludes the use of presently available RDC-based approaches.

5. Experimental

5.1. NMR spectroscopy

Spectra were recorded at 30°C . This is a condition for which a bicelle mixture of dimyristoylphosphatidylcholine (DMPC) and dihexanoylphosphatidylcholine (DHPC), doped with cetyltrimethylammonium bromide (CTAB), was aligned against an external magnetic field and leads to a 10 Hz residual quadrupolar splitting in the ^2H NMR spectrum of HDO. A Varian INOVA500 spectrometer, operating at a ^1H frequency of 499.84 MHz, was used to record the spectra. For the magic angle experiments to record TROSY spectra and to determine ^{15}N CSA tensor, we used a Varian gHX NanoProbe with a ^1H -detection coil and with X tuned for ^{15}N . The sample spinning rate was set to 2.6 kHz so that the torque that aligns the bicelles against the magnetic field was eliminated [21,26]. The ^1H - ^{15}N dipolar couplings were obtained from ^1H - ^{15}N IPAP-HSQC spectra [11]. The ^1H - ^{15}N TROSY spectra [14,36] were collected in the isotropic and anisotropic states with and without the application of magic angle sample spinning, respectively. The sample solution contained 0.5 mM ^{15}N -labeled ubiquitin dissolved in 50 mM sodium phosphate, pH 6.4, 2 mM EDTA, and 7.5% (w/v) DMPC:DHPC:CTAB bicelles. The same ubiquitin solution was used for all experiments. The acquisition times for data collection in the t_1 and t_2 dimensions were 111 and 128 ms, respectively, with matrices of $200 (t_1, ^{15}\text{N}) \times 1024 (t_2, ^1\text{H})$ complex points. All data were processed using the NMRpipe program

software packages [37]. The final processed data, after zero-filling, has a digital resolution of 2.0 Hz and 0.88 Hz for the ^1H and ^{15}N dimensions, respectively.

Peak positions were determined by fitting ellipsoids to each of the experimental contours between 60 and 80% of the peak maximum using the program PIPP [38]. The center of each ellipsoid provides a measure of the experimental peak position; therefore, the center values, obtained for all contours in the 60–80% intensity range of a given peak, were averaged to provide the peak position.

5.2. Alignment tensor calculations

The values for the alignment tensors obtained from the alignment-induced TROSY chemical shift changes, $\Delta\delta_{\text{TROSY}}$, and the values for the error evaluations were calculated using a C-program, which included published subroutines [39] and written in-house. Alignment tensors were calculated using the experimental data and ubiquitin reference structures; the dipolar-refined NMR structure [23] and the X-ray structure [22]. In using the X-ray structure, protons were added using the program MOLMOL [40]. The effect of experimental uncertainties on the TROSY chemical shifts was evaluated using iterative singular value decomposition (SVD) calculations [18] for each dataset. The datasets were generated by adding Gaussian noise to the experimental values. Gaussian noise was assumed to be distributed with a relative probability of $\exp(-x^2/2\sigma^2)$, where x is the experimental value and σ is the rms noise estimated from the pairwise rms deviation between successive measurements of the TROSY chemical shifts. Structural noise was simulated by reorienting the NH bond vectors in a random manner [24]. The deviations between the original and the reoriented vectors are described as a cone having a 5° tilt angle from the original orientation. For the structural noise simulation, the tilt angles between the original and reoriented NH vectors were assumed to be in a Gaussian distribution, $\exp(-\alpha^2/2\theta^2)$, where α is the tilt angle and θ is the assumed standard deviation for a tilt angle of 5° . The transverse rotation angle of the reoriented vector was distributed equally within the cone. If the rmsd between the experimental data and the simulated values was less than 2.55 Hz, the values obtained by simulation were retained. The threshold value of 2.55 Hz gave 68% acceptance rate for the simulated values, thus it represents one standard deviation of the mean.

Acknowledgments

This work was supported by the Japan New Energy and Industrial Technology Development Organization (NEDO). S.T. thanks the Inamori Foundation and the

Novartis Foundation for financial support during the initial stage of this work.

References

- [1] A. Bax, G. Kontaxis, N. Tjandra, Dipolar couplings in macromolecular structure determination, *Methods Enzymol.* 339 (2001) 127–174.
- [2] J.H. Prestegard, H.M. al Hashimi, J.R. Tolman, NMR structures of biomolecules using field oriented media and residual dipolar couplings, *Q. Rev. Biophys.* 33 (2000) 371–424.
- [3] J.H. Prestegard, A.I. Kishore, Partial alignment of biomolecules: an aid to NMR characterization, *Curr. Opin. Chem. Biol.* 5 (2001) 584–590.
- [4] J.H. Prestegard, H. Valafar, J. Glushka, F. Tian, Nuclear magnetic resonance in the era of structural genomics, *Biochemistry* 40 (2001) 8677–8685.
- [5] N. Tjandra, Establishing a degree of order: obtaining high-resolution NMR structures from molecular alignment, *Struct. Fold. Des.* 7 (1999) R205–R211.
- [6] N. Tjandra, J.G. Omichinski, A.M. Gronenborn, G.M. Clore, A. Bax, Use of dipolar ^1H – ^{15}N and ^1H – ^{13}C couplings in the structure determination of magnetically oriented macromolecules in solution, *Nat. Struct. Biol.* 4 (1997) 732–738.
- [7] G.M. Clore, D.S. Garrett, R-factor, Free R, and complete cross-validation for dipolar coupling refinement of NMR structures, *J. Am. Chem. Soc.* 121 (1999) 9008–9012.
- [8] J. Evenas, V. Tugarinov, N.R. Skrynnikov, N.K. Goto, R. Muhandiram, L.E. Kay, Ligand-induced structural changes to maltodextrin-binding protein as studied by solution NMR spectroscopy, *J. Mol. Biol.* 309 (2001) 961–974.
- [9] J.A. Lukin, G. Kontaxis, V. Simplaceanu, Y. Yuan, A. Bax, C. Ho, Quaternary structure of hemoglobin in solution, *Proc. Natl. Acad. Sci. USA* 100 (2003) 517–520.
- [10] F. Cordier, A.J. Dingley, S. Grzesiek, A doublet-separated sensitivity-enhanced HSQC for the determination of scalar and dipolar one-bond J-couplings, *J. Biomol. NMR* 13 (1999) 175–180.
- [11] M. Ottiger, F. Delaglio, A. Bax, Measurement of J and dipolar couplings from simplified two-dimensional NMR spectra, *J. Magn. Reson.* 131 (1998) 373–378.
- [12] J.R. Tolman, J.M. Flanagan, M.A. Kennedy, J.H. Prestegard, Nuclear magnetic dipole interactions in field-oriented proteins: information for structure determination in solution, *Proc. Natl. Acad. Sci. USA* 92 (1995) 9279–9283.
- [13] M. Goldman, Interference effects in the relaxation of a pair of unlike spin one-half nuclei, *J. Magn. Reson.* 60 (1984) 437–452.
- [14] K. Pervushin, R. Riek, G. Wider, K. Wüthrich, Attenuated T_2 relaxation by mutual cancellation of dipole–dipole coupling and chemical shift anisotropy indicates an avenue to NMR structures of very large biological macromolecules in solution, *Proc. Natl. Acad. Sci. USA* 94 (1997) 12366–12371.
- [15] G. Kontaxis, G.M. Clore, A. Bax, Evaluation of cross-correlation effects and measurement of one-bond couplings in proteins with short transverse relaxation times, *J. Magn. Reson.* 143 (2000) 184–196.
- [16] D. Yang, R.A. Venters, G.A. Mueller, W.Y. Choy, L.E. Kay, TROSY-based HNC0 pulse sequences for the measurement of ^1HN – ^{15}N , ^{15}N – ^{13}CO , ^1HN – ^{13}CO , ^{13}CO – ^{13}Ca and ^1HN – ^{13}Ca dipolar couplings in ^{15}N , ^{13}C , ^2H -labeled proteins, *J. Biomol. NMR* 14 (1999) 333–343.
- [17] A. Saupe, Recent results in the field of liquid crystals, *Angew. Chem. Int. Ed. Engl.* 7 (1968) 97–112.
- [18] J.A. Losonczi, M. Andrec, M.W. Fischer, J.H. Prestegard, Order matrix analysis of residual dipolar couplings using singular value decomposition, *J. Magn. Reson.* 138 (1999) 334–342.
- [19] M. Ottiger, A. Bax, Determination of relative N–H^N, N–C', C^a–C', and C^a–H^a effective bond lengths in a protein by NMR in a dilute liquid crystalline phase, *J. Am. Chem. Soc.* 120 (1998) 12334–12341.
- [20] D. Sitkoff, D.A. Case, Theories of chemical shift anisotropies in proteins and nucleic acids, *Prog. NMR spectrosc.* 32 (1998) 165–190.
- [21] J. Kurita, H. Shimahara, N. Utsunomiya-Tate, S. Tate, Measurement of ^{15}N chemical shift anisotropy in a protein dissolved in a dilute liquid crystalline medium with the application of magic angle sample spinning, *J. Magn. Reson.* 163 (2003) 163–173.
- [22] S. Vijay-Kumar, C.E. Bugg, W.J. Cook, Structure of ubiquitin refined at 1.8 Å resolution, *J. Mol. Biol.* 194 (1987) 531–544.
- [23] G. Cornilescu, J. Marquardt, M. Ottiger, A. Bax, Validation of protein structure from anisotropic carbonyl chemical shifts in a dilute liquid crystalline phase, *J. Am. Chem. Soc.* 120 (1998) 6836–6837.
- [24] M. Zweckstetter, A. Bax, Evaluation of uncertainty in alignment tensors obtained from dipolar couplings, *J. Biomol. NMR* 23 (2002) 127–137.
- [25] T.M. Barbara, Cylindrical demagnetization fields and microprobe design in high-resolution NMR, *J. Magn. Reson.* A109 (1994) 265–269.
- [26] J. Courtieu, J.P. Bayles, B.M. Fung, Variable angle sample spinning NMR in liquid crystals, *Prog. NMR spectrosc.* 26 (1994) 141–169.
- [27] N. Tjandra, S.E. Feller, R.W. Pastor, A. Bax, Rotational diffusion anisotropy of human ubiquitin from ^{15}N NMR relaxation, *J. Am. Chem. Soc.* 117 (1995) 12562–12566.
- [28] D. Fushman, N. Tjandra, D. Cowburn, Direct measurement of ^{15}N chemical shift anisotropy in solution, *J. Am. Chem. Soc.* 120 (1998) 10947–10952.
- [29] J. Boyd, C. Redfield, Characterization of ^{15}N chemical shift anisotropy from orientation-dependent changes to ^{15}N chemical shifts in dilute bicelle solutions, *J. Am. Chem. Soc.* 121 (1999) 7441–7442.
- [30] G. Cornilescu, A. Bax, Measurement of proton, nitrogen, and carbonyl chemical shielding anisotropies in a protein dissolved in a dilute liquid crystalline, *J. Am. Chem. Soc.* 122 (2000) 10143–10154.
- [31] Y. Hiyama, C.H. Niu, J.V. Silverton, A. Bavoso, D.A. Torchia, Determination of ^{15}N chemical shift tensor via ^{15}N – ^2H dipolar coupling in Boc-glycylglycyl[^{15}N glycine]benzyl ester, *J. Am. Chem. Soc.* 110 (1988) 2378–2383.
- [32] D.K. Lee, R.J. Wittebort, A. Ramamoorthy, Characterization of ^{15}N chemical shift and ^1H – ^{15}N dipolar coupling interactions in a peptide bond of uniaxially oriented and polycrystalline samples by one-dimensional dipolar chemical shift solid-state NMR spectroscopy, *J. Am. Chem. Soc.* 120 (1998) 8868–8874.
- [33] T.G. Oas, C.J. Hartzell, T.J. McMahon, G.P. Drobny, F.W. Dahlquist, The carbonyl carbon-13 chemical shift tensors of five peptides determined from nitrogen-15 dipole-coupled chemical shift powder patterns, *J. Am. Chem. Soc.* 109 (1987) 5956–5962.
- [34] J. Fiaux, E.B. Bertelsen, A.L. Horwich, K. Wüthrich, NMR analysis of a 900 K GroEL GroES complex, *Nature* 418 (2002) 207–211.
- [35] M. Salzmann, K. Pervushin, G. Wider, H. Senn, K. Wüthrich, NMR assignment and secondary structure determination of an octameric 110 kDa protein using TROSY in triple resonance experiments, *J. Am. Chem. Soc.* 122 (2000) 7543–7548.
- [36] J. Weigelt, Single scan, sensitivity- and gradient-enhanced TROSY for multidimensional NMR experiments, *J. Am. Chem. Soc.* 120 (1998) 10778–10779.

- [37] F. Delaglio, S. Grzesiek, G.W. Vuister, G. Zhu, J. Pfeifer, A. Bax, NMRPipe: a multidimensional spectral processing system based on UNIX pipes, *J. Biomol. NMR* 6 (1995) 277–293.
- [38] D.S. Garrett, R. Powers, A.M. Gronenborn, G.M. Clore, A common sense approach to peak picking in two-, three-, and four-dimensional spectra using automatic computer analysis of contour diagrams, *J. Magn. Reson.* 95 (1991) 214–220.
- [39] W.H. Press, S.A. Teukolsky, W.T. Vetterling, B.P. Flannery, *Numerical Recipes in C*, second ed., Cambridge University Press, New York.
- [40] R. Koradi, M. Billeter, K. Wüthrich, MOLMOL: a program for display and analysis of macromolecular structures, *J. Mol. Graph.* 14 (1996) 51–55.
- [41] L.K. Lee, M. Rance, W.J. Chazin, A.G. Palmer III, Rotational diffusion anisotropy of proteins from simultaneous analysis of ^{15}N and ^{13}C alpha nuclear spin relaxation, *J. Biomol. NMR* 9 (1997) 287–298.
- [42] G.M. Clore, M.R. Starich, A.M. Gronenborn, Measurement of residual dipolar couplings of macromolecules aligned in the nematic phase of a colloidal suspension of rod-shaped viruses, *J. Am. Chem. Soc.* 120 (1998) 10571–10572.